Waveform Comparison - Ring Laser vs. STS-2 Broadband Seismometer

Estimation of Backazimuth and Love Wave Phase Velocity

Page 1 - Event Information

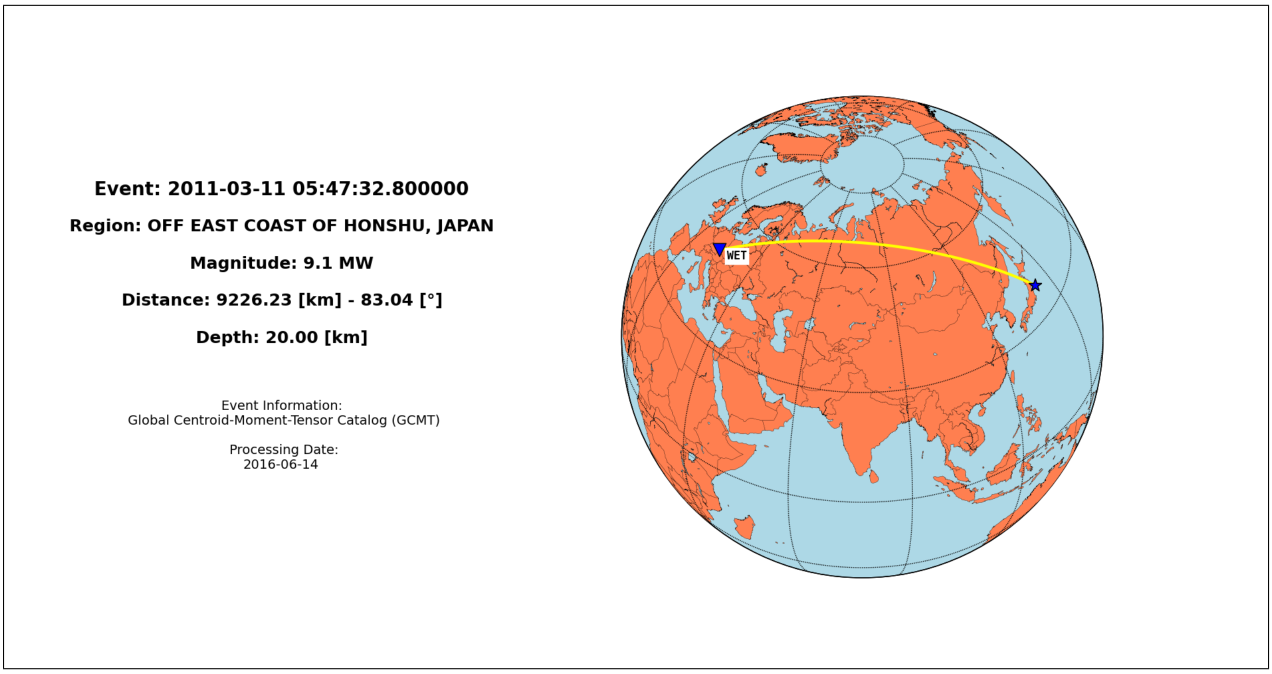

Figure 1: Page 1 - Event Information

The first page shows a map on which the source and receiver locations are indicated. The epicenter of the source is marked by a blue star, while the marker for the receiver station is a blue triangle with the shortcut of the station's name next to it. The scale of the map depends on the source-receiver distance to allow for higher resolution for local events.
On the left side, registered event information is displayed:

- origin time in the format YYYY-mm-dd [T] HH:MM:SS
- Flinn-Engdahl region
- moment magnitude of the earthquake
- epicentral distance (distance between epicenter and receiver station in km and degrees)
- depth of the earthquake (distance between epicenter and hypocenter)

In the last lines, the source of the event information data is specified.

Page 2 - Waveform Comparison

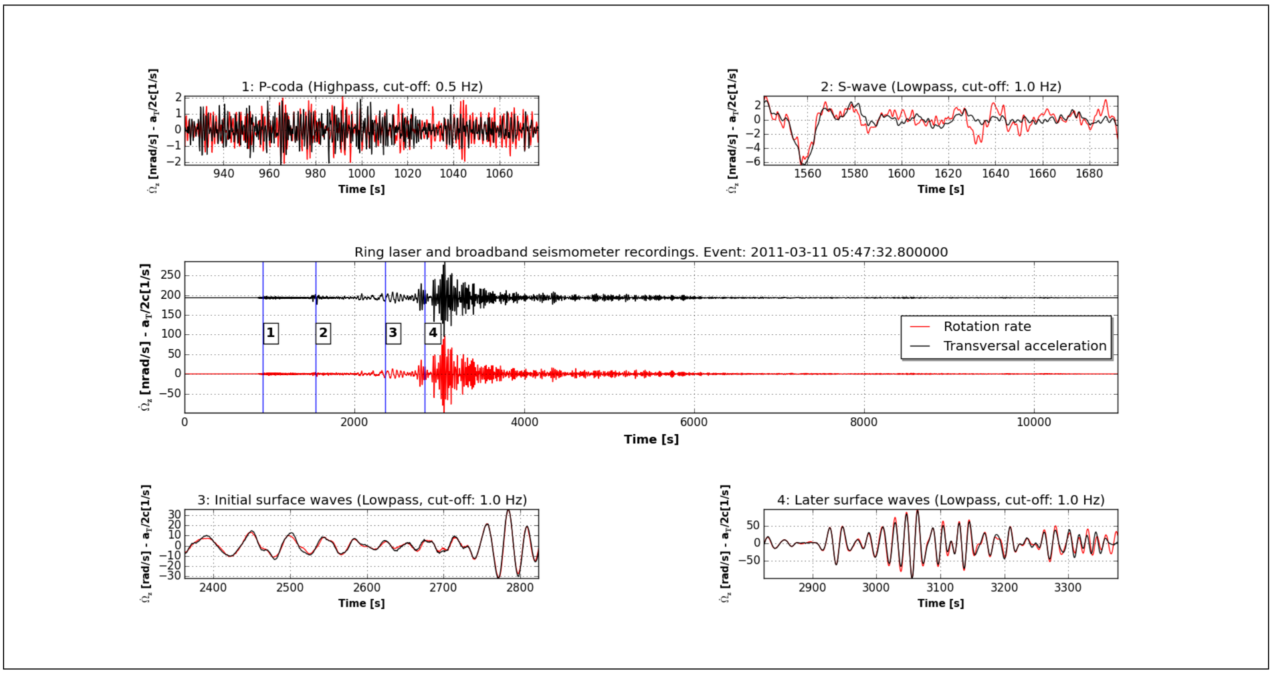

Figure 2: Page 2 - Recordings

The recordings of the ring laser (red) and the broadband seismometer (black) are displayed on this page. The central plot shows the complete traces that were extracted from seismometer/ring laser recordings at the specified station. The surrounding four windows represent short time intervals cropped from the trace to distinguish between different parts of the signal. The start times of these windows are plotted as consecutively numbered vertical lines in the central plot and indicate arrival times of the following wave types (Note: the arrival times were not picked by hand, so they may vary):

1. P-wave (P-Coda)
2. S-wave
3. Initial surface waves
4. Later surface waves

Each signal (rotation rate, acceleration) is detrended linearly, rotation rate units are converted to $\frac{nrad}{s}$. Instrument responses are removed and horizontal acceleration is derived from the particle velocity measurements. Eventually, the signals are low-pass filtered at a certain cutoff-frequency and resampled, depending on the epicentral distance of the event:

Zone	Distance range	Lowpass cutoff	Resampling (decimation factor)
close events	0 km $\leq$ d $\leq$ 333.33 km	4 Hz	2
local events	333.34 km $\leq$ d $\leq$ 1111.11 km	2 Hz	2
teleseismic events	d $>$ 1111.11 km	1 Hz	4 (P-coda by factor 2)

Also for teleseismic events a bandstop-filter (5s<f<12s) is applied to wipe out the secondary microseism noise-band. For displaying the transverse acceleration, we need to rotate the broadband signal from N-/E-components to radial and transverse components. In order to achieve this, the N-/E-components are rotated by the theoretical backazimuth (source direction angle), calculated from the source-receiver geometry.

Rotation rate (red) and transverse acceleration (black) are shown in the subplots. The resemblance/coherence of the waveforms depends on the quality of the signals (influenced by magnitude, source-receiver distance, depth) and the accuracy of the theoretical backazimuth.

Page 3 - Velocity and Backazimuth Estimation

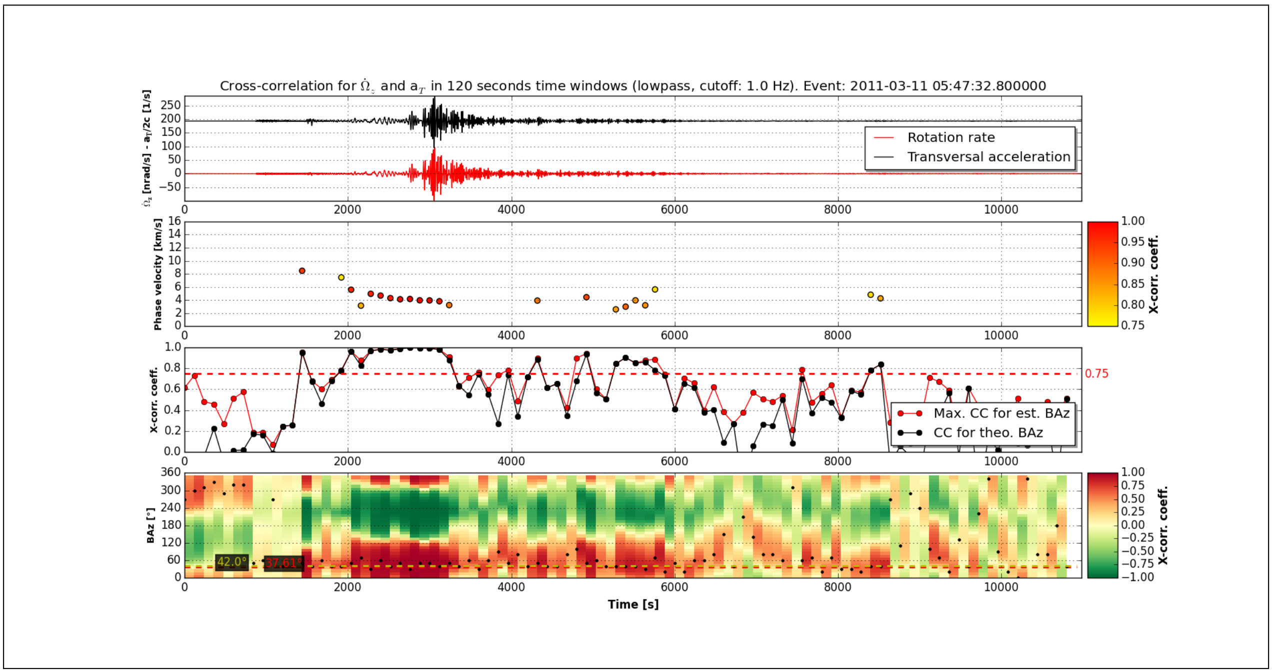

Figure 3: Page 3 - Estimation of Love Wave Phase Velocities and Backazimuth

Results of the comparison of broadband and rotational signal are shown on this page. The relation between rotation rate and transverse acceleration is used to estimate phase velocities in the signal [cf. *Igel et al.* (2005)]:

$$v_{ph} = \frac{1}{2} \cdot \frac{\alpha_T}{\dot{\Omega}_z} \tag{1}$$

In addition, the backazimuth (BAz) is re-evaluated to cross-check the reliability of the theoretical estimation with an estimation from the seismometer/ring laser recordings.
The first plot is adopted from the second page and contains the deduced transverse acceleration (black) and the rotation rate (red) of the station recordings.
In order to evaluate the backazimuths and phase velocities, the recordings are divided into sub-intervals whose length depends on the epicentral distance:

Zone	Interval length
close events	3 s
local events	5 s
non-local events	120 s

For each time interval a correlation between transverse acceleration and rotation rate is computed and displayed in the third subplot. Only if this correlation coefficient for a time window exceeds a threshold of 0.75, a **phase velocity** value is calculated according to equation (1) using the theoretical BAz for rotating the horizontal accelerations (second subplot with a color scale indicating the coefficient value).
In order to calculate the best fitting BAz from the observed signals, a grid search optimization algorithm is employed:
Essentially, in each interval the program loops through 360° in backazimuth test steps (10° each). In each loop, the algorithm performs a cross-correlation to calculate correlation coefficients (CC) between the rotation rate measurements (ring laser) and the transverse acceleration (broadband seismometer) that is rotated from N-/E-component to radial/transverse by the test step values.

The 36 correlation coefficients are plotted column-wise (one column per time interval) in subplot 4, where red fields mark high (positive) correlation, while green ones mark anti-correlation for the associated BAz rotation angle and yellow represents no correlation of the signals. Maximum correlation coefficients of each time interval are displayed as black dots on the respective BAz-field. For comparison, these maximum CCs are also plotted in subplot 3 (red dotted line).
In a last step, the routine is re-run for a smaller BAz step-size of 1° and shorter time-windows (30 s) to calculate a more precise estimate of the backazimuth (plotted as yellow dashed line). The estimated BAz value is averaged not over the BAz of all time windows, but only over those for which a CC> 0.9 could be gained. For comparison, the theoretical BAz is denoted by a red dashed line.

Page 4 - P-Coda Evaluation

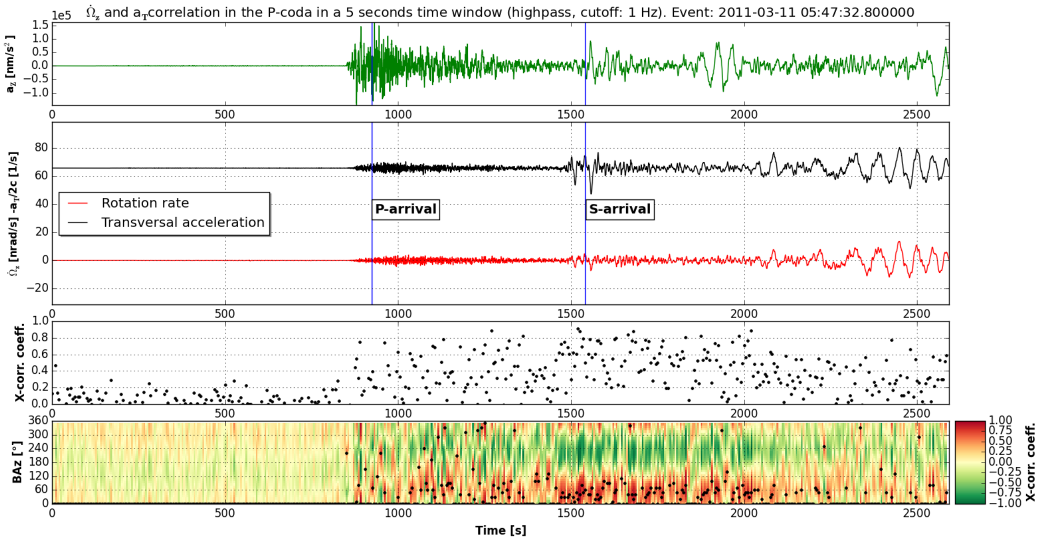

Figure 4: Page 4 - Backazimuth Estimation of the P-coda

The last page deals particularly with the backazimuth analysis of the P-coda [cf. *Pham et al.*(2009)]. In that context, an interval length of 2 s is used for the cross-correlation windows in the BAz determination algorithm.

The uppermost plot shows a time series with the Z-component recordings of the broadband seismometer for the first part of the event. For the same interval, the rotation rate (red) and transverse acceleration (black) are displayed in the second subplot. P- and S-wave arrivals are indicated by vertical lines (not picked by hand).
For this period, the backazimuth values are estimated via grid search optimization analogous to the processing before, but at a higher resolution (2 s-windows).
The correlation coefficients associated with rotation around the theoretical BAz for each 2 s-interval are plotted in the third plot (black dots), while the estimated backazimuths (with correlation-coefficients) can be found in the lowermost figure. In this plot, black dots mark all the BAz values associated with correlation coefficients larger than 50%.

JSON-file

In the .json-file, processed data is stored for post-processing. The file contains the following information:

- data source information (client, network, station, ...)
- event identification
- start- and endtime
- station location (latitude, longitude)
- epicentral distance)
- moment magnitude
- source depth
- peak transverse acceleration
- peak transverse displacement
- peak vertical acceleration
- peak rotation rate
- peak correlation coefficient
- frequency at peak vertical rotation rate
- theoretical backazimuth
- estimated backazimuth
- maximum correlation coefficient for estimated BAz
- SNR of transverse acceleration
- SNR of vertical acceleration
- SNR of vertical rotation rate
- mean phase velocities for 8 frequency bands (0.01-0.02 Hz, 0.02-0.04 Hz, 0.04-0.1 Hz, 0.1-0.2 Hz, 0.2-0.3 Hz, 0.3-0.4 Hz, 0.4-0.6 Hz, 0.6-1 Hz)
- standard deviations for these phase velocities

References:

IGEL, H., U. Schreiber, A. Flaws, B. Schubert, A. Velikoseltsev, and A. Cochard (2005), *Rotational Motions induced by the M8.1 Tokashi-oki Earthquake, September 25, 2003*, Geophys. Res. Lett. **32**, L08309.

PHAM, N. D., H. Igel, J. Wassermann, M. Käser, J. de la Puente, and U. Schreiber (2009), *Observations and Modeling of Rotational Signals in the P-Coda: Constraints on Crustal Scattering*, Bull. Seismol. Soc. Am., **99**, 1315-1332.